

# COLE-COLE ANALYSIS OF THE SUPERSPIN GLASS SYSTEM



O. PETRACIC<sup>a,\*</sup>, S. SAHOO<sup>a</sup>, CH. BINEK<sup>a</sup>, W. KLEEMANN<sup>a</sup>,  
J. B. SOUSA<sup>b</sup>, S. CARDOSO<sup>c</sup> and P. P. FREITAS<sup>c</sup>

<sup>a</sup>*Laboratorium für Angewandte Physik,*

*Gerhard-Mercator-Universität Duisburg, 47048 Duisburg, Germany*

<sup>b</sup>*IFIMUP, Departamento de Fisica,*

*Universidade de Porto, 4169-007 Porto, Portugal*

<sup>c</sup>*INESC, Rua Alves Redol 9-1, 1000 Lisbon, Portugal*

(Received )

## Abstract

Ac susceptibility measurements were performed on discontinuous magnetic multilayers [ $\text{Co}_{80}\text{Fe}_{20}(t)/\text{Al}_2\text{O}_3(3\text{nm})]_{10}$ ,  $t = 0.9$  and  $1.0 \text{ nm}$ , by Superconducting Quantum Interference Device (SQUID) magnetometry. The CoFe forms nearly spherical ferromagnetic single-domain nanoparticles in the diamagnetic  $\text{Al}_2\text{O}_3$  matrix. Due to dipolar interactions and random distribution of anisotropy axes the system exhibits a spin-glass phase. We measured the ac susceptibility as a

---

\*Corresponding author: Tel. +49-203-379-2939; fax: +49-203-379-1965, email: petracic@kleemann.uni-duisburg.de

function of temperature  $20 \leq T \leq 100$  K at different *dc* fields and as a function of frequency  $0.01 \leq f \leq 1000$  Hz. The spectral data were successfully analysed by use of the phenomenological Cole-Cole model, giving a power-law temperature dependence of the characteristic relaxation time  $\tau_c$  and a high value for the polydispersivity exponent,  $\alpha \approx 0.8$ , typical of spin glass systems.

*Keywords:* Multilayers, Ac susceptibility, Polydispersivity, Dipolar interactions, Spin glass behavior

## INTRODUCTION

The dynamic and static magnetic properties of spin glasses (SG) are still a subject of intense experimental and theoretical research. In the field of experiments a vast variety of different spin glass systems (Young, 1997) have yet been found and investigated. A rather new class are the so-called superspin glass (SSG) systems (Kleemann, Petracic, Binek, Kakazei *et al.*, 2001). Here the sample is composed of an ensemble of dipolarly interacting nanoparticles, each having a superspin moment in the order of  $1000 \mu_B$ . The spin glass properties are due to frustration, a natural property of dipolar interaction, and to randomness of the anisotropy axis directions, frequently also of the spin sizes. Two different types of realisations of SSG systems exist, frozen ferrofluids (Dormann, Fiorani and Tronc, 1997; Dormann, Fiorani, Cherkaoui, Tronc *et al.*, 1999; Djurberg, Svedlindh, Nordblad, Hansen *et al.*, 1997; Mamiya, Nakatani and Furubayashi, 1999) and discontinuous magnetic multilayers (Sankar, Dender, Borchers, Smith *et al.*, 2000; Sousa, Kakazei, Pogorelov, Santos *et al.*, 2001; Kleemann, Petracic, Binek, Kakazei *et al.*, 2001; Petracic, Kleemann, Binek, Kakazei *et al.*, 2002; Sahoo, Petracic, Binek, Kleemann *et al.*, 2002a).

It is widely accepted that 3-dimensional (3D) nanoparticle systems with high enough density of the particles and sufficiently narrow particle size dis-

tribution do have spin glass properties, i.e. there exists a phase transition temperature,  $T_g$ , where the characteristic relaxation time and the static non-linear susceptibility diverge (Djurberg, Svedlindh, Nordblad, Hansen *et al.*, 1997; Kleemann, Petracic, Binek, Kakazei *et al.*, 2001; Petracic, Kleemann, Binek, Kakazei *et al.*, 2002; Sahoo, Petracic, Binek, Kleemann *et al.*, 2002a). In order to observe SSG properties the collective glass temperature,  $T_g$ , has to be larger than the so-called blocking temperature,  $T_b$ , at which the relaxation time of the individual moments (Néel, 1949; Brown, 1963)

$$\tau = \tau_0 \exp(KV/k_B T), \quad (1)$$

reaches the order of the timescale of the experiment. Here  $K$  is the effective anisotropy constant of one nanoparticle,  $V$  the volume and  $\tau_0 \sim 10^{-10}$ s the relaxation time at  $T \rightarrow \infty$ . Below  $T_b$  the particle moments are "blocked".

The condition  $T_g < T_b$  is met in our discontinuous metal-insulator multilayers (DMIMs)  $[\text{Co}_{80}\text{Fe}_{20}(t)/\text{Al}_2\text{O}_3(3\text{nm})]_n$ , where  $t \leq 1.0$  nm is the nominal thickness of the ferromagnetic CoFe layers and  $n$  the number of bilayers. The CoFe does not form a continuous layer but forms nearly spherical particles embedded in the diamagnetic  $\text{Al}_2\text{O}_3$  matrix (Kakazei, Pogorelov, Lopes, Sousa *et al.*, 2001). One finds self-organized arrangements of particles in each layer (Stappert, Dumpich, Sahoo, Petracic *et al.*, 2002), i.e. the inter-particle distances are nearly constant. While SSG behavior is found for relatively small values of  $t \leq 1.0$  nm and  $n = 10$  (Kleemann, Petracic, Binek, Kakazei *et al.*, 2001; Petracic, Kleemann, Binek, Kakazei *et al.*, 2002; Sahoo, Petracic, Binek, Kleemann *et al.*, 2002a), for higher values of the nominal thickness,  $1.0 < t \leq 1.4$  nm, superferromagnetism (SFM) is observed (Kleemann, Petracic, Binek, Kakazei *et al.*, 2001; Sahoo, Sichelschmidt, Petracic, Binek *et al.*, 2002b; Chen, Sichelschmidt, Kleemann, Petracic *et al.*, 2002).

In this article we will focus on the SSG systems  $[\text{Co}_{80}\text{Fe}_{20}(t)/\text{Al}_2\text{O}_3(3\text{nm})]_{10}$ , with  $t = 0.9$  and  $1.0$  nm. The existence of a spin glass phase was evidenced by means of dynamic criticality, static criticality of the

non-linear susceptibility and dynamical scaling (Kleemann, Petracic, Binek, Kakazei *et al.*, 2001; Petracic, Kleemann, Binek, Kakazei *et al.*, 2002; Sahoo, Petracic, Binek, Kleemann *et al.*, 2002a). All three methods yield convincing values for the glass transition temperature and the dynamical critical exponents, respectively,  $T_g \approx 44$  K,  $z\nu \approx 9.5$ ,  $\gamma \approx 1.47$  and  $\beta \approx 1.0$  for  $t = 0.9$  nm and  $T_g \approx 49$  K,  $z\nu \approx 10.0$ ,  $\gamma \approx 1.36$  and  $\beta \approx 0.6$  for  $t = 1.0$  nm.  $T_g$  and  $z\nu$  are the error weighted average values obtained from different methods.

While  $z\nu$  characterizes the divergence of the relaxation time of the largest ordered cluster as  $T \rightarrow T_g$ , there is a wide distribution of shorter relaxation times due to non-percolating clusters. They are characteristic of the glassy nature of the system and deserve a focused investigation, which will be described in the present paper. To this end we analyse the results of measurements of the complex *ac* susceptibility carried out at different *ac* amplitudes and bias fields and frequencies  $f$ . In particular the so-called Cole-Cole presentation,  $\chi''$  vs  $\chi'$ , will be discussed in terms of appropriate empirical models of relaxational polydispersivity.

## EXPERIMENTAL

The DMIM samples Glass/Al<sub>2</sub>O<sub>3</sub>(3nm)/[Co<sub>80</sub>Fe<sub>20</sub>( $t$ )/ Al<sub>2</sub>O<sub>3</sub>(3nm)]<sub>10</sub> ( $t = 0.9$  and 1.0 nm) are prepared by sequential Xe ion beam sputtering from two separate targets (Kakazei, Pogorelov, Lopes, Sousa *et al.*, 2001). The CoFe forms nearly spherical granules of approximately 3 nm diameter and 2 nm inter-particle spacing as found from transmission electron microscopy (TEM) studies (Stappert, Dumpich, Sahoo, Petracic *et al.*, 2002).

The measurements were performed by use of a commercial Superconducting Quantum Interference Device (SQUID) magnetometer (MPMS-5S, Quantum Design). The *ac* susceptibility,  $\chi = \chi' - i\chi''$ , is extracted from the linear response of the sample on an oscillating *ac* field,  $\mu_0 H_{ac} = 0.05$  or 0.4 mT at different *ac* frequencies,  $0.01 \leq f \leq 1000$  Hz. The constant *dc*

field was either  $\mu_0 H = (0 \pm 0.03)$  mT or  $(0.6 \pm 0.1)$  mT.

## RESULTS AND DISCUSSION

Figure 1 shows the real  $\chi'$  and the imaginary parts  $\chi''$  of the *ac* susceptibility vs temperature  $T$  for the samples  $t = 0.9$  nm (a) and  $1.0$  nm (b) under four different conditions. Curves 1 and 1' are measured at the *ac* frequency  $f = 0.1$  and curves 2 and 2' at  $1$  Hz, whereas for curves 1 and 2 an *ac* field amplitude of  $\mu_0 H_{ac} = 0.05$  mT and a *dc* field of  $\mu_0 H = 0$  mT were applied. For curves 1' and 2' an *ac* field amplitude of  $\mu_0 H_{ac} = 0.4$  mT and a *dc* field of  $\mu_0 H = 0.6$  mT were used (see Figure 2 for an illustration). For both samples a similar behavior is encountered. Both the increase of the probing *ac* field amplitude and the application of a bias field result in a suppression of the amplitude of the real part  $\chi'(T)$  and a shift  $\Delta T_m$  of the peak to higher temperatures. Quantitatively the shift is  $\Delta T_m(1' - 1) = 2.2$  (3.8) K and  $\Delta T_m(2' - 2) = 2.3$  (3.6) K for  $t = 0.9$  (1.0) nm, respectively. The imaginary part  $\chi''(T)$  is also suppressed, but the inflection point at  $T_f$  is shifted to lower temperatures,  $\Delta T_f(1' - 1) = -6.0$  (-10.1) K and  $\Delta T_f(2' - 2) = -6.2$  (-8.2) K for  $t = 0.9$  (1.0) nm, respectively. This behavior is well known from other SG systems and model calculations (Canella and Mydosh, 1972; Barbara, Malozemoff and Imry, 1981) and can be explained in terms of a competition between the non-critical linear susceptibility and the critical non-linear susceptibility. In other words, the suppression of both the real and the imaginary parts reflects the obvious fact that the  $M(H)$  curve becomes increasingly non-linear when increasing the *ac* amplitude and/or the bias field (see Fig. 2).

Next we studied the frequency spectra,  $\chi'(f)$  and  $\chi''(f)$ . Figure 3 and Fig. 4 ( $t = 0.9$  and  $1.0$  nm respectively) show the real  $\chi'$  (a) and the imaginary part  $\chi''$  (b) as functions of the *ac* frequency  $f$  for different temperatures  $T = 45, 50, 55$  and  $60$  K in zero-field and  $\mu_0 H_{ac} = 0.05$  mT. While some negative

curvature still indicates a well-defined dispersion step at  $f > 10^3$  Hz for  $T > 60$  K, this step becomes gradually broadened as  $T$  decreases. At low  $T$  the real parts show nearly constant negative slopes, thus corresponding to an extremely broad dispersion step. The imaginary parts reveal extremely broad peaks, which strongly shift to lower frequencies with decreasing temperature. Obviously our SSG system exhibits a very wide distribution of relaxation times with a pronounced temperature dependence.

A satisfactory description of the data is provided by the phenomenological Cole-Cole model (Cole and Cole, 1941; Jonscher, 1983) and was successfully applied e.g. to 2-dimensional (2D) (Dekker, Arts, de Wijn and van Duyneveldt, 1989; Hagiwara, 1998) or pseudo-1-dimensional SG systems (Ravindran, Rubenacker, Haines and Drumheller, 1989). The complex *ac* susceptibility,  $\chi = \chi' - i\chi''$ , is written in the Cole-Cole model as (Jonscher, 1983)

$$\chi(\omega) = \chi_s + \frac{\chi_0 - \chi_s}{1 + (i\omega\tau_c)^{1-\alpha}}, \quad (2)$$

where  $\chi_0$  and  $\chi_s$  are the isothermal (low-f) and adiabatic (high-f) susceptibilities, respectively,  $\tau_c$  is the characteristic relaxation time and  $\alpha$  a measure of the polydispersivity of the system. The case  $\alpha = 0$  yields the standard Debye-type relaxator with one single relaxation frequency, as found, e.g., in the case of a monodisperse ensemble of non-interacting superparamagnetic particles obeying Eq. 1. The limiting case  $\alpha = 1$  corresponds to an infinitely wide distribution of relaxation times. In SG systems one expects values of  $\alpha$  near to 1.

After decomposing Eq. 2 into its real and imaginary parts it is possible to perform a fit to the data as shown in Fig. 3 and 4. One finds (compare to Dekker *et al.*, 1989; Ravindran *et al.*, 1989)

$$\chi'(\omega) = \chi_s + \frac{\chi_0 - \chi_s}{2} \left( 1 - \frac{\sinh[(1-\alpha)\ln(\omega\tau_c)]}{\cosh[(1-\alpha)\ln(\omega\tau_c)] + \cos[\frac{1}{2}(1-\alpha)\pi]} \right) \quad (3)$$

$$\chi''(\omega) = \frac{\chi_0 - \chi_S}{2} \left( \frac{\sin[\frac{1}{2}(1-\alpha)\pi]}{\cosh[(1-\alpha)\ln(\omega\tau_c)] + \cos[\frac{1}{2}(1-\alpha)\pi]} \right), \quad (4)$$

where  $\omega = 2\pi f$ . Best results are obtained, when fitting to the imaginary part  $\chi''(f)$ , since only three parameters,  $\chi_0 - \chi_S$ ,  $(1 - \alpha)$  and  $\tau_c$  are needed in this case.

Figure 5 shows the results from the fitting,  $\tau_c$  (open circles) and  $\alpha$  vs  $T$  (open diamonds) for both samples,  $t = 0.9$  (a) and  $1.0$  nm (b). One finds that the characteristic relaxation time  $\tau_c$  is increasing with decreasing temperature. It changes by eight (a) or ten orders (b) of magnitude, respectively. By this kind of extraction of  $\tau_c$  one has access to an extremely wide timescale and is, hence, more advantageous compared to the standard method of extracting  $\tau_c$  from the  $\chi'(T)$  data. It is straightforward to perform a fit of the  $\tau_c(T)$  data to a critical power-law, which was already used in previous publications (Kleemann, Petracic, Binek, Kakazei *et al.*, 2001; Petracic, Kleemann, Binek, Kakazei *et al.*, 2002),  $\tau_c = \tau_0(T/T_g - 1)^{-z\nu}$  (solid line). It yields reasonable results, but the value of  $z\nu$  must be kept restricted or even fixed to  $z\nu = 9$ . Then we obtain  $\tau_0 = (5.0 \cdot 10^{-8} \pm 5.1 \cdot 10^{-8})$  s,  $T_g = (42.63 \pm 0.18)$  K and  $z\nu = 9.0 \pm 0.7$  ( $t = 0.9$  nm) and  $\tau_0 = (3.46 \cdot 10^{-8} \pm 2.1 \cdot 10^{-10})$  s,  $T_g = (43.9354 \pm 0.0002)$  K and  $z\nu = 9$  fixed ( $t = 1.0$  nm), respectively. In the case of  $t = 0.9$  nm the values for  $T_g$  and  $\tau_0$  correspond well to the values obtained previously (Kleemann, Petracic, Binek, Kakazei *et al.*, 2001; Petracic, Kleemann, Binek, Kakazei *et al.*, 2002). This does not apply to the  $t = 1.0$  nm sample, where  $T_g \approx 44$  K differs strongly from the value shown above,  $T_g \approx 49$  K. Interestingly the Cole-Cole fit to the  $T = 45$  K data for  $t = 1.0$  nm does not converge (encircled data points in Fig. 5 (b)) leading to the conclusion that the data emerge from the non-ergodic regime,  $T < T_g$ . It is worth to mention that the fit to the modified power law according to (Souletie and Tholence, 1985),  $\tau_c = \tau_0(1 - T_g/T)^{-z\nu}$ , (broken line) yields similar values, i.e.  $\tau_0 = (2.67 \cdot 10^{-9} \pm 2.9 \cdot 10^{-9})$  s,  $T_g = (43.19 \pm 0.11)$  K and  $z\nu = 9.0$  fixed ( $t = 0.9$  nm) and  $\tau_0 = (3.4 \cdot 10^{-10} \pm 6.2 \cdot 10^{-10})$  s,  $T_g = (44.004 \pm 0.036)$  K and  $z\nu = 10$  fixed ( $t = 1.0$  nm), respectively. It is

not possible to judge about the advantage of this method here.

The exponent  $\alpha$  increases, as expected, with decreasing temperature (Fig. 5. Its high value ( $\alpha \approx 0.8$ ) meets the expectation, that a SG system should have a very broad distribution of relaxation times (Mydosh, 1993).

Often susceptibility data are presented in a way, where the imaginary part is plotted against the real part (Cole-Cole plot),  $\chi''(\chi')$  (Cole and Cole, 1941; Jonscher, 1983), where a classic Debye-relaxator should yield a perfect semicircle, centered on the  $\chi'$ -axis at  $(\chi_0 + \chi_S)/2$  and with radius  $(\chi_0 - \chi_S)/2$ . The apex of the semi-circle corresponds to  $\omega\tau_c = 1$ . Non-zero  $\alpha$  has the effect to depress the semi-circle such that the angles between the  $\chi'$ -axis and the tangents at  $\omega = 0$  and  $\omega \rightarrow \infty$  are  $\mp(1 - \alpha)\pi/2$ , respectively. Figure 6 shows the susceptibility data for  $t = 0.9$  (a) and 1.0 nm at different temperatures  $T = 45, 50, 55$  and 60 K. The above derived expressions for the real and imaginary parts (Eq. 3 and 4) can be expressed in the form (Hagiwara, 1998)

$$\chi''(\chi') = -\frac{\chi_0 - \chi_S}{2 \tan[(1 - \alpha)\pi/2]} + \sqrt{(\chi' - \chi_S)(\chi_0 - \chi') + \frac{(\chi_0 - \chi_S)^2}{4 \tan^2[(1 - \alpha)\pi/2]}}. \quad (5)$$

The fit yields similar results for  $\alpha(T)$  compared to those from the fit to the imaginary part  $\chi''(f)$  (Fig. 5, solid versus open diamonds). It should be noticed that  $\chi_S = 0$  in all cases, i.e. no measurable response is expected at frequencies above single particle flip frequencies. This corroborates the model of ferromagnetic order within each superparamagnetic particle.

## CONCLUSION

The dynamical susceptibility of the SSG system  $[\text{Co}_{80}\text{Fe}_{20}(t)/\text{Al}_2\text{O}_3(3\text{nm})]_{10}$  ( $t = 0.9$  and 1.0 nm) was studied under the influence of a bias field and in view of its polydispersivity within the framework of a Cole-Cole description. Cole-Cole fits yield reasonable values for the characteristic relaxation time  $\tau_c$  of the system and for its polydispersivity exponent  $\alpha$ . The relaxation

time can be well described by a critical power-law dependence. One should note that by this kind of extraction of  $\tau_c$  one has access to an extremely wide timescale of eight or ten orders of magnitude. Reasonably large values,  $\alpha \approx 0.8$ , are obtained, which are typical of SG systems. The Cole-Cole plots of the susceptibility data confirm the SG characteristic, i.e. one observes a strongly flattened semi-circle.

### ***Acknowledgements***

The authors acknowledge financial support by DFG (Graduiertenkolleg "Struktur und Dynamik heterogener Systeme").

### ***References***

- Barbara, B., A. Malozemoff and Y. Imry (1981). Field-dependence of the dc susceptibility of spin glasses. *Physica B & C* **108**, 1289.
- Brown, W. (1963). Thermal fluctuations of a single-domain particle. *Phys. Rev.* **130**, 1677.
- Canella, V. and J. Mydosh (1972). Magnetic ordering in gold-iron alloys. *Phys. Rev. B* **6**, 4220.
- Chen, X., O. Sichelschmidt, W. Kleemann, O. Petracic *et al.* (2002). Domain wall relaxation, creep, sliding and switching in superferromagnetic discontinuous Co<sub>80</sub>Fe<sub>20</sub>-Al<sub>2</sub>O<sub>3</sub> multilayers. *Phys. Rev. Lett., submitted*.
- Cole, K. and R. Cole (1941). Dispersion and absorption in dielectrics. *J. Chem. Phys.* **9**, 341.
- Dekker, C., A. Arts, H. de Wijn and A. van Duyneveldt (1989). Activated dynamics in a two-dimensional Ising spin glass: Rb<sub>2</sub>Cu<sub>1-x</sub>Co<sub>x</sub>F<sub>4</sub>. *Phys. Rev. B* **40**, 11243.

- Djurberg, C., P. Svedlindh, P. Nordblad, M. Hansen *et al.* (1997). Dynamics of an interacting particle system: evidence of critical slowing down. *Phys. Rev. Lett.* **79**, 5154.
- Dormann, J., D. Fiorani, R. Cherkaoui, E. Tronc *et al.* (1999). From pure superparamagnetism to glass collective state in  $\gamma$ -Fe<sub>2</sub>O<sub>3</sub> nanoparticle assemblies. *J. Magn. Magn. Mater.* **203**, 23.
- Dormann, J., D. Fiorani and E. Tronc (1997). Magnetic relaxation in fine-particle systems. *Adv. Chem. Phys.* **98**, 283.
- Hagiwara, M. (1998). Cole-Cole plot analysis of the spin-glass system NiC<sub>2</sub>O<sub>4</sub> · 2(2M1z)<sub>0.49</sub>(H<sub>2</sub>O)<sub>0.51</sub>. *J. Magn. Magn. Mater.* **177-181**, 89.
- Jonscher, A. (1983). In *Dielectric relaxation in solids*. Chelsea Dielectrics Press, London.
- Kakazei, G., Y. Pogorelov, A. Lopes, J. Sousa *et al.* (2001). Tunnel magnetoresistance and magnetic ordering in ion-beam sputtered Co<sub>80</sub>Fe<sub>20</sub>/Al<sub>2</sub>O<sub>3</sub> discontinuous multilayers. *J. Appl. Phys.* **90**, 4044.
- Kleemann, W., O. Petracic, C. Binek, G. Kakazei *et al.* (2001). Interacting ferromagnetic nanoparticles in discontinuous Co<sub>80</sub>Fe<sub>20</sub>/Al<sub>2</sub>O<sub>3</sub> multilayers: from superspin glass to reentrant superferromagnetism. *Phys. Rev. B* **63**, 134423.
- Mamiya, H., I. Nakatani and T. Furubayashi (1999). Slow dynamics for spin-glass-like phase of a ferromagnetic fine particle system. *Phys. Rev. Lett.* **82**, 4332.
- Mydosh, J. (1993). In *Spin glasses: an experimental introduction*. Taylor & Francis, London.
- Néel, L. (1949). Théorie du trainage magnétique des ferromagnétiques en grains fins avec applications aux terres cuites. *Ann. Geophys.* **5**, 99.
- Petricic, O., W. Kleemann, C. Binek, G. Kakazei *et al.* (2002). Superspin glass behavior of interacting ferromagnetic nanoparticles in discontinuous magnetic multilayers. *Phase Transitions* **75**, 73.

- Ravindran, K., G. Rubenacker, D. Haines and J. Drumheller (1989). Spin-cluster relaxation times in the spin-glass  $[(\text{CH}_3)_3\text{NH}] \text{Co}_{0.4} \text{Ni}_{0.6}\text{Cl}_3 \cdot 2\text{H}_2\text{O}$ . *Phys. Rev. B* **40**, 9431.
- Sahoo, S., O. Petracic, C. Binek, W. Kleemann *et al.* (2002a). Superspin-glass nature of discontinuous  $\text{Co}_{80}\text{Fe}_{20}/\text{Al}_2\text{O}_3$  multilayers. *Phys. Rev. B* **65**, 134406.
- Sahoo, S., O. Sichelschmidt, O. Petracic, C. Binek *et al.* (2002b). Magnetic states of discontinuous  $\text{Co}_{80}\text{Fe}_{20}-\text{Al}_2\text{O}_3$  multilayers. *J. Magn. Magn. Mater.* **240**, 433.
- Sankar, S., D. Dender, J. Borchers, D. Smith *et al.* (2000). Magnetic correlations in non-percolated Co-SiO<sub>2</sub> granular films. *J. Magn. Magn. Mater.* **221**, 1.
- Souletie, J. and J. Tholence (1985). Critical slowing down in spin glasses and other glasses : Fulcher versus power law. *Phys. Rev. B* **32**, 516.
- Sousa, J., G. Kakazei, Y. Pogorelov, J. Santos *et al.* (2001). Magnetic states of granular layered CoFe-Al<sub>2</sub>O<sub>3</sub> system. *IEEE Trans. Mag.* **37**, 2200.
- Stappert, S., G. Dumpich, S. Sahoo, O. Petracic *et al.* (2002). Transmission electron microscopy studies on ion-beam sputtered  $\text{Co}_{80}\text{Fe}_{20}/\text{Al}_2\text{O}_3$  discontinuous bilayers. *unpublished*.
- Young, A. (1997). (Editor), Spin glasses and random fields. In *Series on directions in condensed matter physics*, Vol. 12. World Scientific, Singapore.

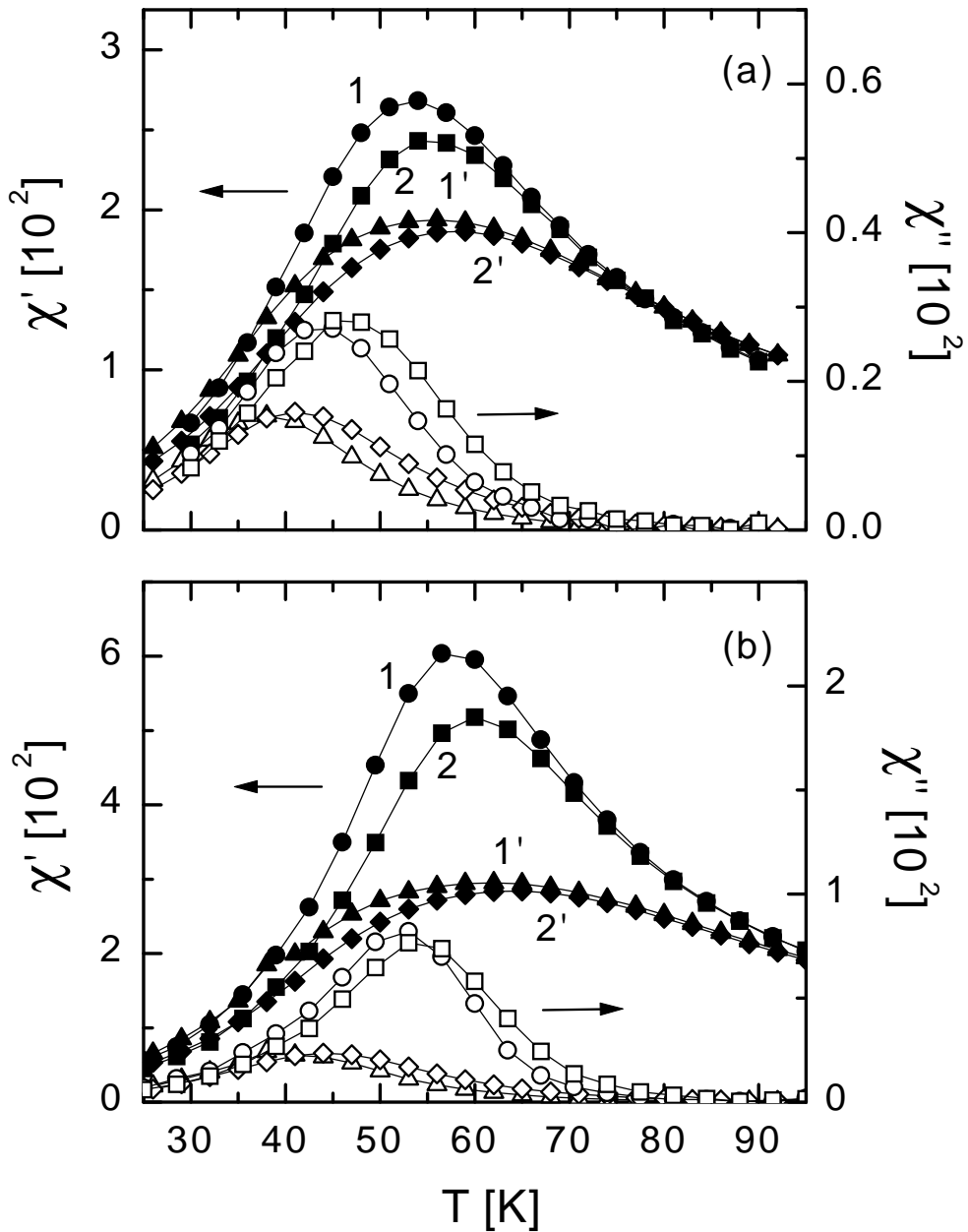


Figure 1:  $\chi'$  and  $\chi''$  vs  $T$  for  $t = 0.9$  nm (a) and  $1.0$  nm (b) measured at constant frequency  $f = 0.1$  (curves 1 and 1') and  $1$  Hz (curves 2 and 2') with  $ac$  field amplitude  $\mu_0 H_{ac} = 0.05$  mT and  $dc$  field  $\mu_0 H = 0$  mT (curves 1 and 2) and  $ac$  field amplitude  $\mu_0 H_{ac} = 0.4$  mT and  $dc$  field  $\mu_0 H = 0.6$  mT (curves 1' and 2'), respectively.

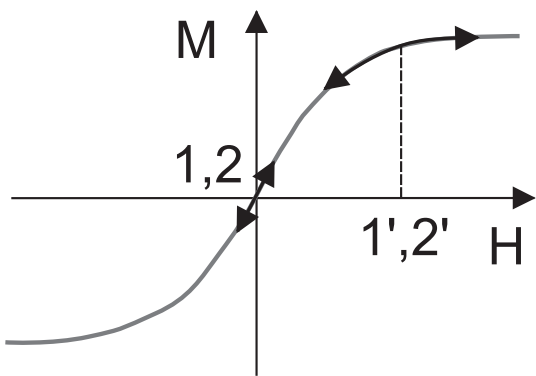


Figure 2: Schematic drawing of the measurement conditions relevant for the data as numbered in Figure 1 (see text). The solid curve shows  $M(H)$  without hysteresis.

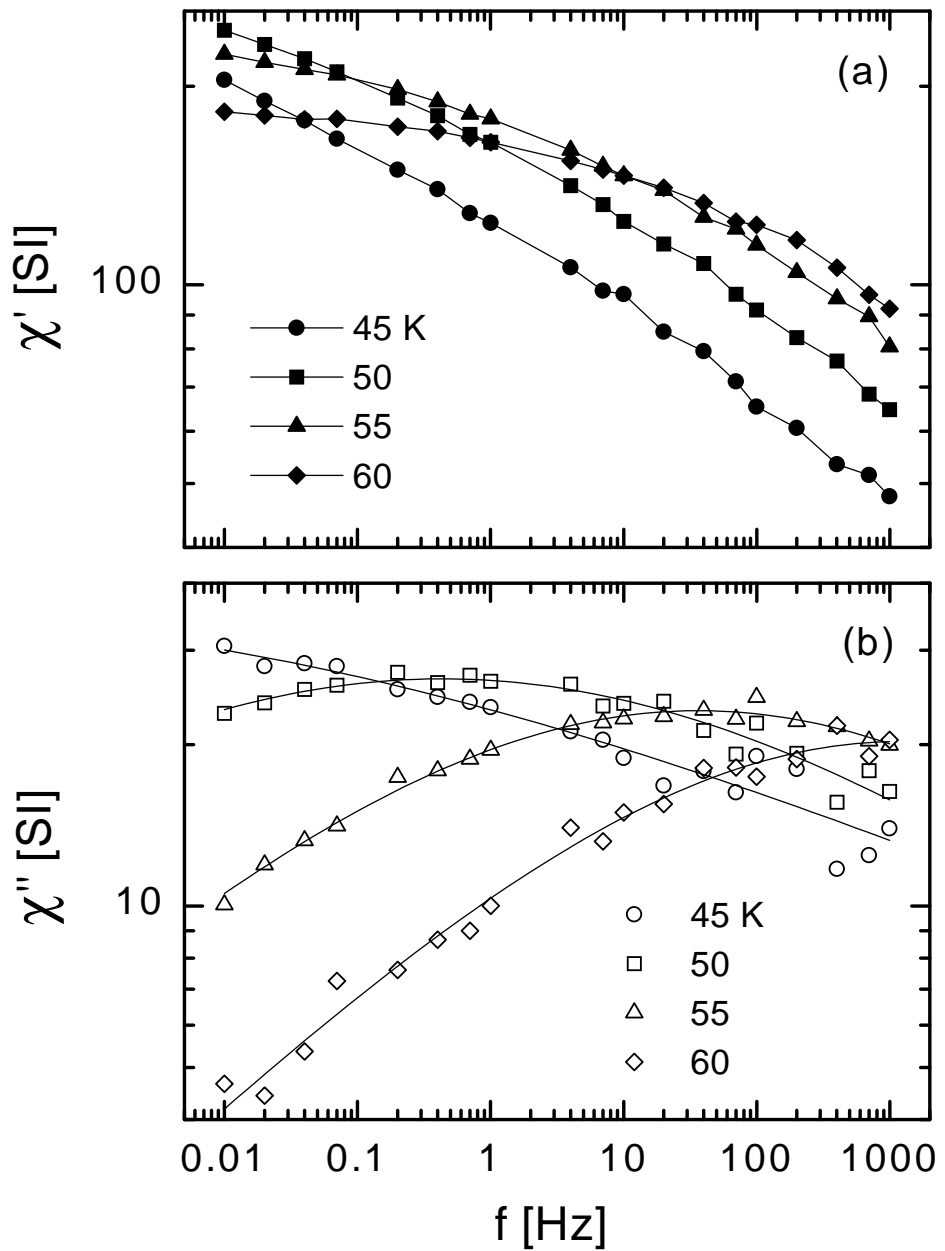


Figure 3:  $\chi'$  (a) and  $\chi''$  (b) vs  $f$  at different temperatures  $T = 45, 50, 55$  and  $60$  K for the  $t = 0.9$  nm sample in zero-field and  $\mu_0 H_{ac} = 0.05$  mT. The lines in (a) are guides to the eyes and in (b) best fits according to Eq. 4.

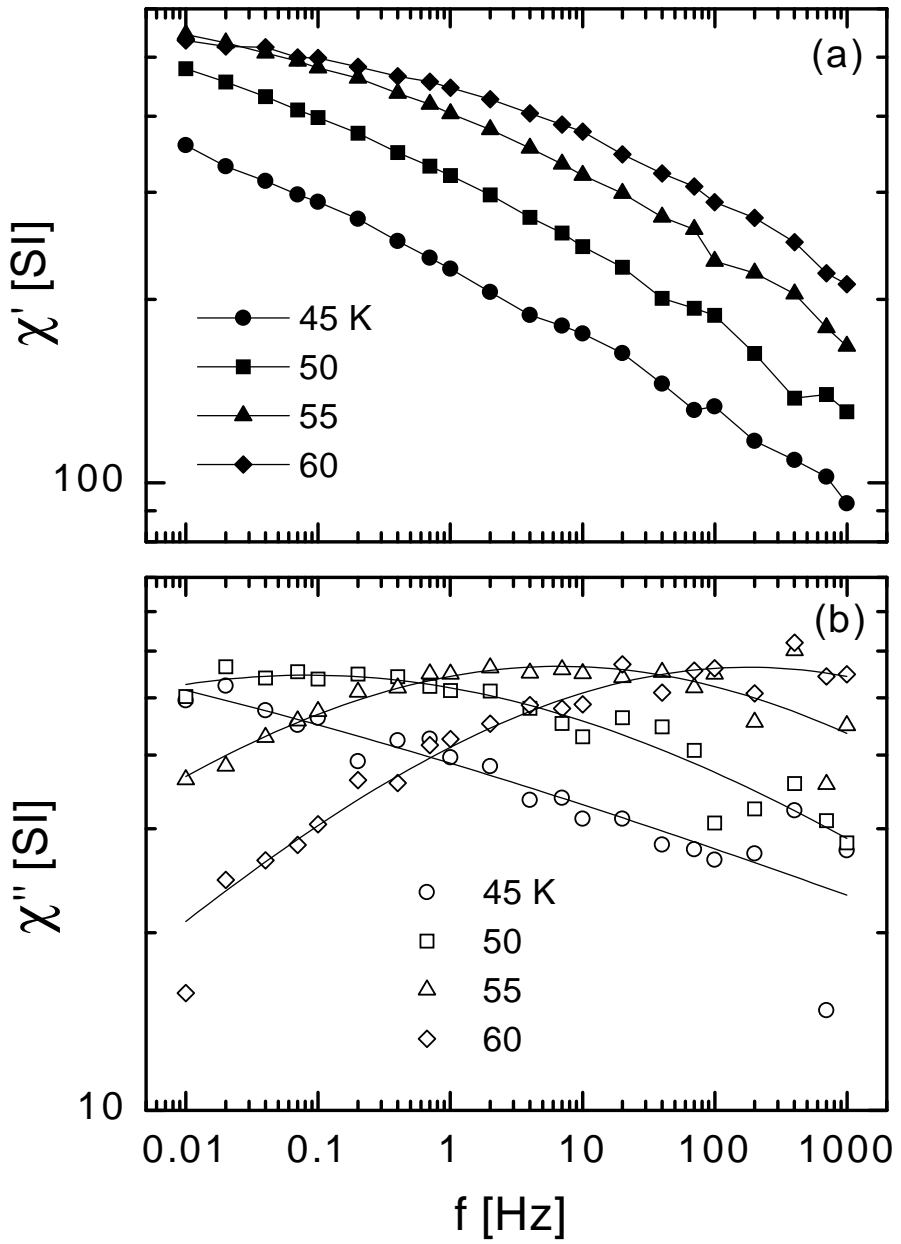


Figure 4:  $\chi'$  (a) and  $\chi''$  (b) vs  $f$  at different temperatures  $T = 45, 50, 55$  and  $60 \text{ K}$  for the  $t = 1.0 \text{ nm}$  sample in zero-field and  $\mu_0 H_{ac} = 0.05 \text{ mT}$ . The lines in (a) are guides to the eyes and in (b) best fits according to Eq. 4.

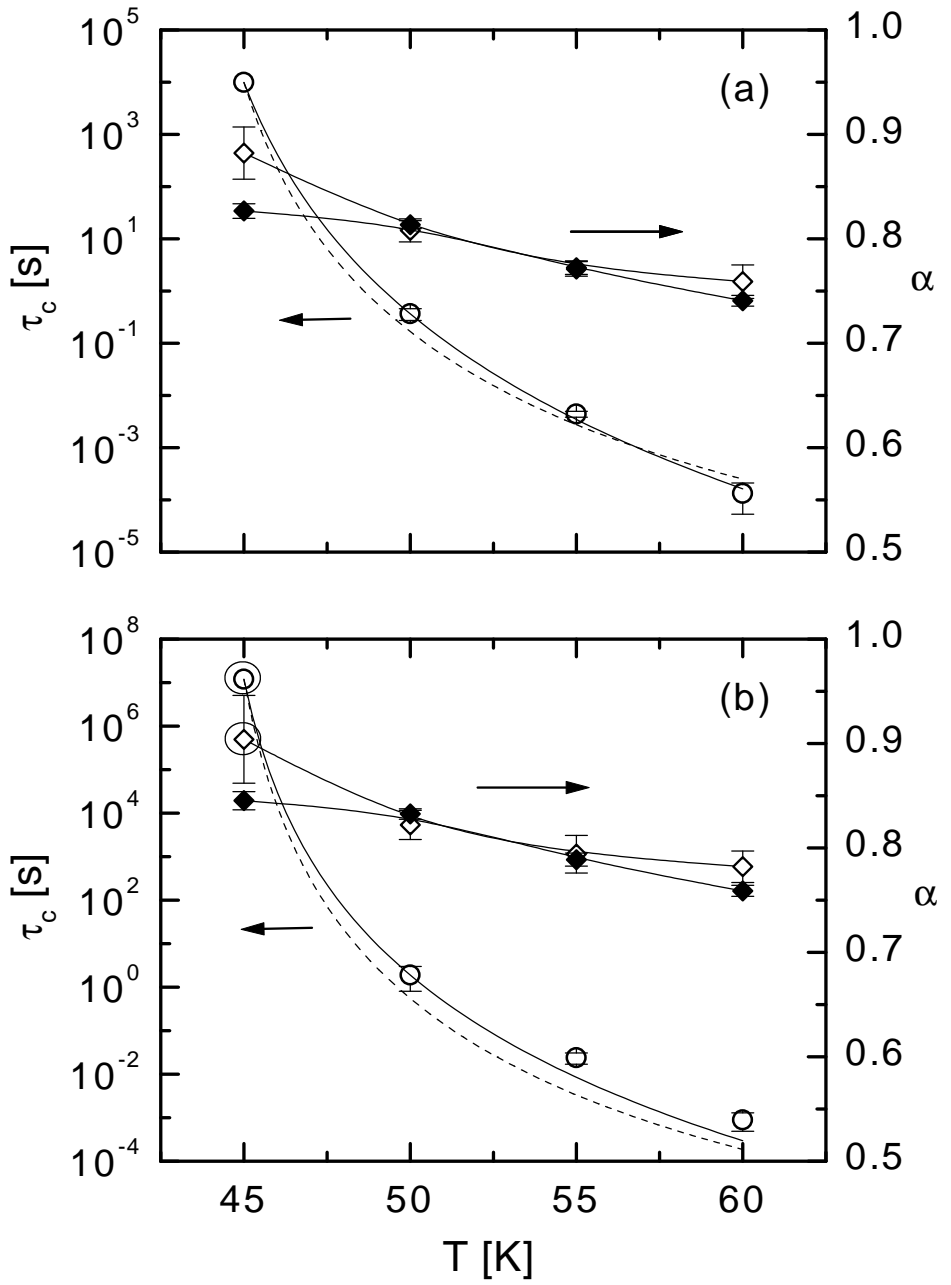


Figure 5: Results from Cole-Cole fits to the data shown in Fig. 3, 4 and 6 for  $t = 0.9$  (a) and  $1.0$  nm (b). The characteristic relaxation times  $\tau_c$  (open circles) are best fitted to a critical power law (solid and broken lines; see text). The polydispersivity exponent  $\alpha$  vs  $T$  as obtained from fits to Eq. 4 (open diamonds) and to Eq. 5 (solid diamonds), respectively, are connected by eye-guiding lines. Encircled data points are results from non-converging fits.

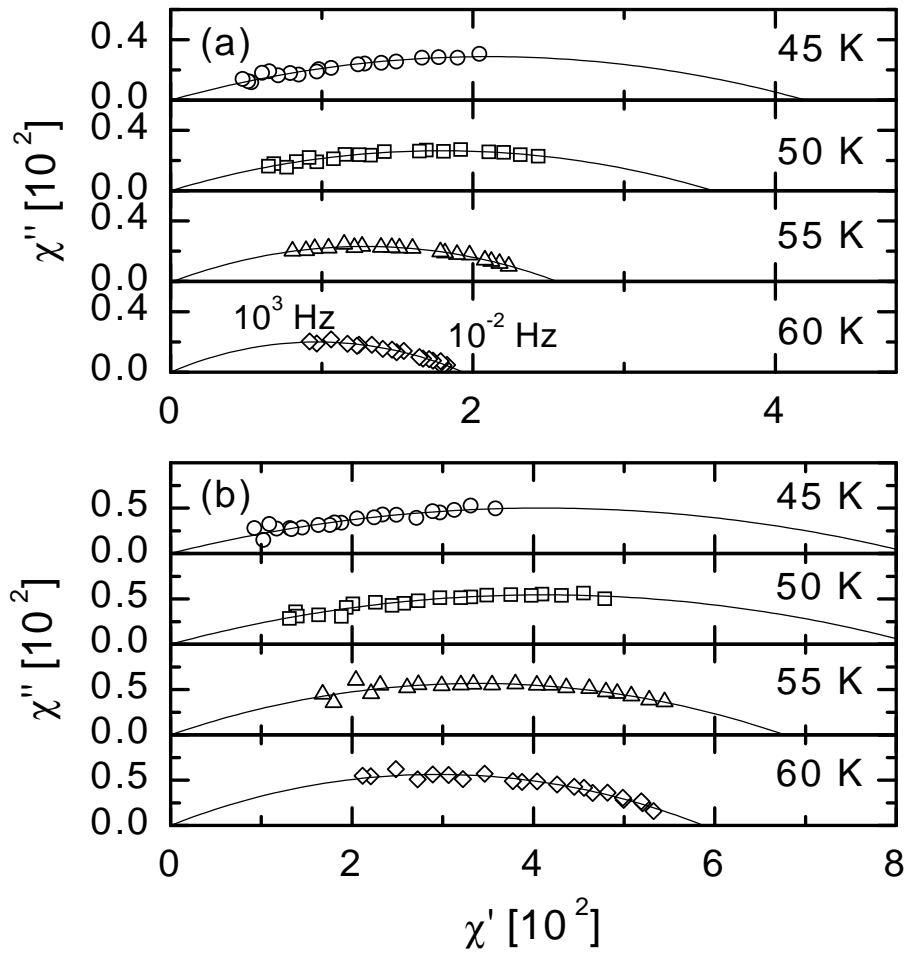


Figure 6: Cole-Cole plots of  $\chi''$  vs  $\chi'$  for  $t = 0.9$  (a) and  $1.0$  nm (b) at different temperatures and frequencies as indicated. The solid lines are best fits according to Eq. 5.